Physica A 390 (2011) 3742–3753

Contents lists available at SciVerse ScienceDirect

Physica A

journal homepage: www.elsevier.com/locate/physa

Myopic random walkers and exclusion processes: Single and multispecies

Kerry A. Landman *, Anthony E. Fernando

Department of Mathematics and Statistics, University of Melbourne, Victoria 3010, Australia

ARTICLE INFO

Article history:
Received 22 December 2010
Received in revised form 6 April 2011
Available online 29 June 2011

Keywords:
Cell motility
Exclusion process
Myopic random walk
Nonlinear diffusion
Multispecies

ABSTRACT

A motility mechanism based on a simple exclusion process, where the probability of movement of an agent depends on the number of unoccupied nearest-neighbor sites is considered. Such interacting agents are termed myopic. This problem is an extension of the famous blind or myopic ant in a labyrinth problem. For the interacting agent models considered here, each agent plays the role of an ant in a labyrinth, where the paths of allowed sites though the labyrinth consist of sites not occupied by other agents. We derive a nonlinear diffusion equation for the average occupancy of the discrete agent-based model for myopic agents. In contrast, interacting blind agents have a constant probability of movement to each of their nearest-neighbor sites, giving rise to a linear diffusion equation. Insight into the various terms in the nonlinear diffusion coefficient is obtained from a study of multiple subpopulations of interacting myopic agents, where an advection–diffusion equation for each subpopulation is derived, and from tracking an individual agent within the crowd, where a motility coefficient is extracted. Averaged discrete simulation data compares very well with the solution to the continuum models. We also compare the behavior of myopic and blind agents. The myopic motility mechanism is biologically motivated to emulate information an individual cell gathers from environment cues. The multispecies model developed and investigated here assists with the interpretation of experimental data involving the tracking subpopulations of cells within a total cell population.

1. Introduction

Lattice-based interacting random walk models where agents move and each lattice site is occupied by at most one agent are known as exclusion processes [1,2]. Such models are used in many application areas such as traffic flow [3], ecological applications [4] and cellular tumor invasion [5].

Random walk simulations of a crowd of agents readily provide information at two spatial scales. Microscopic data can be obtained by tagging and tracking the movement of individual agents within the population [6–8]. The rules of movement and the interactions between the agents will influence the mean displacement and mean square displacement of the agent. Macroscopic data can be obtained by averaging simulation data over many realizations – this yields an average density distribution as a function of spatial position. If this is repeated at different times, a spatio-temporal picture of the density distribution emerges [7,9].

Recently there has been much interest in taking agent-based rules, writing these as transition probabilities and deriving a continuum description of the system in terms of a partial differential equation (PDE) [1,9–14]. It is well known

* Corresponding author. Tel.: +61 3 83446762; fax: +61 3 83444599.
E-mail address: kerryl@unimelb.edu.au (K.A. Landman).

0378-4371/$ – see front matter © 2011 Elsevier B.V. All rights reserved.
doi:10.1016/j.physa.2011.06.034

that symmetric exclusion processes (without bias) gives a linear diffusion equation [1]. Various biologically motivated mechanisms, accounting for contact-forming, contact-breaking and contact-maintaining interactions have been considered within the framework of an exclusion process [8,10,12]. Such processes give rise to a nonlinear diffusion equation. Some contact interactions lead to a nonlinear diffusion function which is negative for some density values. In these cases, the PDE models may give rise to solutions containing shocks [15,16].

Here we consider an extension of the famous blind or myopic ant in a labyrinth problem [17–20]. In the original problem, a single ant performs a random walk on a random network, where there may be some inaccessible or forbidden nearest-neighbor sites. A blind ant attempts to move to any of its nearest-neighbor sites, but only moves to sites on the random network are allowed – therefore, many attempted moves are aborted. Alternatively, a myopic ant attempts to move to permitted sites only – in this case there are no aborted moves. We use these ideas to describe and analyze a lattice-based motility model which takes account of the number of unoccupied sites which are accessible to the agent. We consider a crowd of myopic agents. For each agent, the positions of all the other agents are forbidden (but, of course, only ones in the nearest neighborhood are relevant at each move). Therefore, the set of unoccupied sites plays the role of the labyrinth. Since all agents are allowed to move at each time step, the labyrinth can change at each time step. We derive transition probabilities for the movement of interacting myopic agents. Averaging the site occupancy gives a nonlinear diffusion equation, where the diffusivity is always positive. We compare the results for myopic agents with those for blind agents previously investigated [9].

In order to appreciate the form of the diffusion function for a myopic population, it is informative to study subpopulations of agents [9,11]. We derive a nonlinear advection–diffusion equation for each subpopulation. If all subpopulations are identical, we are able to uncover a relationship between the diffusion and advection functions for the subpopulations and the diffusion function for a single population. Moreover, we will show that the multispecies diffusion term can be related back to the mean square displacement of an individual tagged agent. This provides an appreciation of the way the spatial scales are integrated into the system.

We define the discrete model and use conservation of mass arguments to construct a PDE describing the average occupancy of the discrete model for both single and multiple species of agents. We also derive the mean square displacement of a single agent in a crowd of agents. We compare the average simulation results to the solution of the PDE and show they match well. Finally, we comment on the source of errors, the usefulness of the multispecies approach to understand the behavior of a single species of agents, and the implications to cell biology.

2. Discrete model

Motile agents move on an arbitrary d-dimensional periodic lattice with uniform spacing Δ. Agents occupy sites on the lattice. This is equivalent to agents residing in regions, since each site v is associated with a spatial region consisting of all points closer to site v than to any other. In two dimensions, these regions are polygonal tiles; the square lattice is associated with square tiles, while the triangular lattice is associated with hexagonal tiles. We consider an exclusion process [21], so that each site can either be occupied by a single agent or be unoccupied.

For any site v on a periodic lattice, we define the nearest neighborhood set $\mathcal{N}\{v\}$ as the set of nearest-neighbor sites, that is, those sites one lattice-space distant from v. In the model these are the sites to which movements from site v can be attempted. The number of nearest neighbors of site v is $N = |\mathcal{N}\{v\}|$.

A simple exclusion process [1,2] with random sequential updating [21] is implemented on the periodic lattice. If there are M agents on the lattice, then for each time step of duration τ, we make M sequential independent random choices of an agent. On average, each agent is chosen once per time step. When chosen, an agent is given the opportunity to move with probability P. Although on average each agent is chosen once per time step, some agents may be selected more than once and some not at all. The relationship between the simulation time and real time is governed by P, the probability that an agent will move a distance Δ within time τ. Therefore, setting $P = 1$ means that agents have the opportunity to move a distance Δ within time τ.

We define blind and myopic agents, which execute different types of random walks.

(1) **Blind agents.** The agent attempts to move to one of the N nearest-neighbor sites with equal probability P/N. Naturally, in an exclusion process, if the randomly chosen target site is occupied, the move is aborted.
(2) **Myopic agents.** Suppose at least one of $\mathcal{N}\{v\}$ is unoccupied. The agent attempts to move to one of the $N - k$ unoccupied nearest-neighbor sites ($k = 0, 1, \ldots, N - 1$) with equal probability $P/(N - k)$. The agent cannot move only when all sites in $\mathcal{N}\{v\}$ are occupied.

A myopic agent never attempts a move to an occupied site, and so no move is aborted. These definitions are extensions to the ones used for a blind or myopic ant in a labyrinth problem [17–20]. Now the set of unoccupied sites plays the role of the labyrinth. For our problem, the labyrinth can change at each time step. Here, we are interested in investigating the behavior of a crowd of myopic agents and comparing that to the behavior of a crowd of blind agents.

3. Conservation equation and continuum model

We use standard conservation arguments to derive a continuum model [1,9,12]. The key steps in connecting our discrete model with a continuum model are outlined here. We denote the occupancy of site v as C_v, with $C_v = 1$ for an occupied site

and $C_v = 0$ for an empty site. Many statistically identical realizations are averaged to give an average occupancy of site v, denoted as $\langle C_v \rangle$. This quantity represents a local probability of occupancy or a local density.

3.1. Single species

The change in average occupancy of site v during the time interval t to $t + \tau$ is denoted $\delta\langle C_v \rangle$. We let $T(v'|v)$ be the conditional transition probability that the agent will move from site v to site $v' \in \mathcal{N}\{v\}$ during τ. Then the change in average occupancy due to a transition in a given direction is $T(v'|v)\langle C_v \rangle$. Summing over all directions, we obtain the discrete conservation equation

$$\delta\langle C_v \rangle = \sum_{v' \in \mathcal{N}\{v\}} \left[T(v|v')\langle C_{v'} \rangle - T(v'|v)\langle C_v \rangle \right]. \tag{1}$$

Changes in average occupancy due to transitions into site v have a positive sign, while transitions out of site v have a negative sign. Since each factor in Eq. (1) is interpreted as a probability, we are assuming that the occupancy of a lattice site is independent of the occupancy of other lattice sites [1]. A similar assumption is implicit in developing $T(v'|v)$ appropriate for blind and myopic walkers below.

For **blind walkers**, there are no agent interactions apart from exclusion. The conditional transition probability $T(v'|v)$ is just the probability P/N of moving to any of the target sites v' multiplied by the probability that the destination site v' is vacant. Therefore,

$$T(v'|v) = \frac{P}{N}(1 - \langle C_{v'} \rangle). \tag{2}$$

For **myopic walkers**, the probability of transitioning from v to $v' \in \mathcal{N}\{v\}$ depends on how many sites are unoccupied. To this end, we define $\mathcal{O}_k^j\{v\}$ to be a set containing exactly k nearest-neighbor sites from the possible $N - 1$ sites in the set $\mathcal{N}\{v\} \setminus \{v'\}$. The superscript j denotes the $\binom{N-1}{k}$ possible choices of k distinct elements in $\mathcal{O}_k^j\{v\}$. We denote by $\mathcal{U}_k^j\{v\}$ the set containing the other $N - 1 - k$ nearest-neighbor sites, namely, the complement $(\mathcal{N}\{v\} \setminus \{v'\}) \setminus \mathcal{O}_k^j\{v\}$. We define such sets for each value of $k = 0, 1, \ldots, N - 1$. Then we can write

$$T(v'|v) = (1 - \langle C_{v'} \rangle) \sum_{k=0}^{N-1} \frac{P}{N-k} \left[\sum_{j=1}^{\binom{N-1}{k}} \prod_{u \in \mathcal{O}_k^j\{v\}} \langle C_u \rangle \prod_{w \in \mathcal{U}_k^j\{v\}} (1 - \langle C_w \rangle) \right]. \tag{3}$$

Since a myopic agent at v attempts to move to one of the $N-k$ unoccupied nearest-neighbor sites ($k = 0, 1, \ldots, N-1$) with equal probability $P/(N-k)$, the term in square parentheses represents the probability that there are exactly k occupied and $N - 1 - k$ unoccupied sites in $\mathcal{N}\{v\} \setminus \{v'\}$, accounting for $\binom{N-1}{k}$ choices of this configuration. The summation in k accounts for all possible choices of the number of occupied sites. Note, when either $\mathcal{O}_k^j\{v\}$ or $\mathcal{U}_k^j\{v\}$ is empty, then the product terms are taken to be unity.

The discrete model is related to a PDE in the appropriate limit as $\Delta \to 0$ and $\tau \to 0$, where the discrete values of $\langle C_v \rangle$ are replaced by a continuous variable C. To do this, all terms in Eq. (1) are expanded in Taylor series about the particular site v, keeping terms up to $\mathcal{O}(\Delta^2)$. The truncated Taylor series are substituted into Eq. (1), and the expression is divided by τ. Taking limits as $\Delta \to 0$ and $\tau \to 0$ jointly, with the ratio Δ^2/τ held constant [22,23], in the continuum limit we obtain a nonlinear diffusion equation of the form

$$\frac{\partial C}{\partial t} = D_0 \nabla \cdot (\mathcal{D}(C) \nabla C). \tag{4}$$

Here, the free agent diffusivity is

$$D_0 = \frac{P}{2d} \lim_{\Delta, \tau \to 0} \left(\frac{\Delta^2}{\tau} \right), \tag{5}$$

where d is the dimension of the lattice.

Using expression Eq. (2) or Eq. (3) for blind and myopic walkers respectively in Eq. (1), the nonlinear diffusion function in Eq. (4) is

$$\mathcal{D}(C) = \begin{cases} 1, & \text{for blind walkers,} \\ 1 + \dfrac{2N}{N-1} \displaystyle\sum_{i=1}^{N-1} C^i - (N+1)C^N, & \text{for myopic walkers.} \end{cases} \tag{6}$$

The expression for myopic walkers can also be written as

$$\mathcal{D}(C) = 1 + \frac{2N}{N-1} \left(\frac{C - C^N}{1 - C} \right) - (N+1)C^N. \tag{7}$$

For blind walkers, the diffusivity is a constant, as expected [1,9]. However, for myopic walkers the form of the diffusivity function is more complex – it depends on the number of nearest-neighbor sites, and therefore is lattice dependent. This means that different continuum models arise from the various common two-dimensional and three-dimensional lattices with the same myopic agent mechanism. Furthermore, $\mathcal{D}(0) = 1$, $\mathcal{D}(1) = N$ and $\mathcal{D}(C) \geq 1$. In fact, $\mathcal{D}(C)$ has a single local maximum in the interval $C \in [0, 1]$. Hence, the diffusivity for a population of myopic agents is always higher than for blind agents, as expected.

To understand the complexity of the form of $\mathcal{D}(C)$, it is informative to look at subpopulations of motile agents. Such an analysis allows us to interpret the terms in $\mathcal{D}(C)$. Furthermore, tagging individual agents and investigating the mean square displacement with time also gives additional insight into the form of $\mathcal{D}(C)$.

3.2. Multiple species

We now consider an exclusion process with m subpopulations. We write down a conservation of occupancy statement for each of these subpopulations $C_v^{(r)}$ $(r = 1, 2, \ldots, m)$ at site v. Now assume that the conditional transition probability that the agent will move from site v to site $v' \in \mathcal{N}\{v\}$ during a time step τ depends only on the occupancy of site v' and not whether v' is occupied by a particular subpopulation or not. For blind and myopic agents, this means that $T^{(r)}(v'|v)$ is the same for each subpopulation, apart from a constant multiplicative factor, and that $T^{(r)}(v'|v)$ is a function of $\sum_{r=1}^{m} C_v^{(r)}$, the total occupancy of a site. By the same arguments as above, we obtain the discrete conservation equation

$$\delta\langle C_v^{(r)}\rangle = \sum_{v' \in \mathcal{N}\{v\}} \left[T^{(r)}(v|v')\langle C_{v'}^{(r)}\rangle - T^{(r)}(v'|v)\langle C_v^{(r)}\rangle \right]. \tag{8}$$

In the appropriate limit, the resulting continuum equations can be written as a system of equations for m subpopulations with density $C^{(r)}$, for each $r = 1, 2, \ldots, m$. Suppose each subpopulation r moves with probability $P^{(r)}$ per time step. Then each subpopulation satisfies a nonlinear advection–diffusion equation

$$\frac{\partial C^{(r)}}{\partial t} = D_0^{(r)} \nabla \cdot \left(D(C) \nabla C^{(r)} + C^{(r)} V(C) \nabla C \right), \quad \text{where } r = 1, 2, \ldots, m, \tag{9}$$

where

$$D_0^{(r)} = \frac{P^{(r)}}{2d} \lim_{\Delta, \tau \to 0} \left(\frac{\Delta^2}{\tau} \right). \tag{10}$$

The first term in parentheses in Eq. (9) is the diffusive flux of subpopulation r, while the second term is the advective flux term of subpopulation r down the gradient of the total agent density (with advective velocity $-V(C)\nabla C$).

Using Eq. (2) or Eq. (3) for blind and myopic walkers respectively in Eq. (8), the nonlinear diffusion and advection function in Eq. (9) are

$$D(C) = \begin{cases} 1 - C, & \text{for blind walkers,} \\ 1 - C^N, & \text{for myopic walkers,} \end{cases} \tag{11}$$

$$V(C) = \begin{cases} 1, & \text{for blind walkers,} \\ \dfrac{2N}{N-1} \displaystyle\sum_{i=0}^{N-2} C^i - NC^{N-1}, & \text{for myopic walkers.} \end{cases} \tag{12}$$

The expression for myopic walkers can also be written as

$$V(C) = \frac{2N}{N-1} \left(\frac{1 - C^{N-1}}{1 - C} \right) - NC^{N-1}. \tag{13}$$

The functions $D(C)$ and $V(C)$ for blind walkers were determined by Simpson et al. [9] and the functions are lattice-independent. However, for myopic walkers, the two functions depend on the number of nearest-neighbor sites, and are therefore lattice dependent. The $D(C)$ is monotonically decreasing to zero, the $V(C)$ is a positive function such that $V(0) = 2N/(N-1)$ and $V(1) = N$. Comparison of the two functions for blind and myopic agents shows that the diffusivity and advective function for a population of myopic agents is always larger than for blind agents, for each value of $0 \leq C \leq 1$. Table 1 gives N for various d-dimensional lattices ($d = 1, 2, 3$), thus providing the nonlinear diffusion function $D(C)$ and advective function $V(C)$ arising from myopic rules.

A relationship between the form of $V(C)$ and $\mathcal{D}(C)$ given by Eqs. (12)–(13) and (6)–(7) respectively can be determined by considering the total population, where all the subpopulations are identical. Then we write $D_0^{(r)} = D_0$ for all r. We can sum the m conservation equations to produce a single equation for the total population C. The resulting equation is the nonlinear diffusion equation appropriate to a single species, namely Eq. (4), when we identify

$$\mathcal{D}(C) = D(C) + CV(C). \tag{14}$$

The form of this decomposition can be further investigated by tagging individual agents and investigating the mean square displacement with time.

Table 1
For lattice dimension d, number of nearest-neighbor sites $N = |\mathcal{N}\{v\}|$ for various lattices needed for $D(C)$ and $V(C)$ in Eqs. (11) and (12).

Lattice	d	N
Linear	1	2
Hexagonal (triangular tiling)	2	3
Simple square	2	4
Triangular (hexagonal tiling)	2	6
Diamond cubic	3	4
Simple cubic	3	6
Body centered cubic – quadrilateral	3	8
Face centered cubic – tetrahedral	3	12
Hexagonal close-packed	3	12

4. Tagged agent in a crowd of agents

Let the position of a tagged agent after n steps be denoted by $\mathbf{R}_n$, where the starting position is $\mathbf{R}_0$. Then the agent displacement after n steps is

$$\mathbf{R}_n - \mathbf{R}_0 = \sum_{j=1}^{n} \mathbf{Y}_j, \tag{15}$$

where $\mathbf{Y}_j$ represents the displacement on the jth step [22].

The expected value of the displacement is zero for agents executing either a blind and myopic walk, so the mean displacement $\langle \mathbf{R}_n - \mathbf{R}_0 \rangle$ after n steps is zero. The mean square displacement of the jth displacement is

$$\langle \mathbf{Y}_j^2 \rangle = T(v'|v)\Delta^2 N, \tag{16}$$

for the N lattice sites $v' \in \mathcal{N}\{v\}$ at a distance Δ from current site v. In the limit as $\Delta \to 0$ and $\tau \to 0$ jointly, with the ratio Δ^2/τ held constant, we require only the dominant term in Eq. (16). This is obtained by replacing $\langle C_v \rangle$ and $\langle C_{v'} \rangle$ for any $v' \in \mathcal{N}\{v\}$ with the continuous variable C, giving

$$T(v'|v) \sim \begin{cases} \dfrac{P}{N}(1-C), & \text{for blind walkers,} \\ (1-C)\displaystyle\sum_{k=0}^{N-1} \frac{P}{N-k} \binom{N-1}{k} (1-C)^{N-1-k} C^k, & \text{for myopic walkers.} \end{cases} \tag{17}$$

The expression for myopic walkers can be simplified as

$$\sum_{k=0}^{N-1} \frac{P}{N-k} \binom{N-1}{k} (1-C)^{N-k} C^k = \frac{P}{N} \sum_{k=0}^{N-1} \binom{N}{k} (1-C)^{N-k} C^k = \frac{P}{N}(1-C^N), \tag{18}$$

from the binomial expansion of $[(1-C)+C]^N$. Now we can identify the expression in Eq. (17) with $PD(C)/N$ using Eq. (11), to obtain the result

$$\langle \mathbf{Y}_j^2 \rangle = \Delta^2 P D(C). \tag{19}$$

Since n steps each of duration τ give the continuous time $t = n\tau$, we have (in the limit as $\Delta, \tau \to 0$ such that Δ^2/τ is a constant),

$$\sum_{l=1}^{n} \langle \mathbf{Y}_j^2 \rangle = n\Delta^2 P D(C) = P\frac{\Delta^2}{\tau} D(C) t = 2dD_0 D(C) t. \tag{20}$$

Without any loss of generality, we determine the horizontal x-component of mean square displacement, denoted MSD_x, by dividing the mean square displacement by the dimension d to give

$$\mathrm{MSD}_x = \left(\frac{\Delta^2}{\tau}\right) \frac{P}{d} D(C) t = 2D_0 D(C) t. \tag{21}$$

The MSD_x of an isolated blind or myopic agent is $2D_0 t$. Therefore the factor $D(C)$ represents the decrease in motility of a single agent as it interacts with a crowd of similarly moving agents. This function is the diffusive interaction term in the decomposition obtained in Eq. (14).

Simulations were performed on large randomly and uniformly seeded regular lattices in d-dimensions ($d = 1, 2, 3$), with spacing $\Delta = 1$, with periodic boundary conditions. The dimensions were chosen so that each domain contained

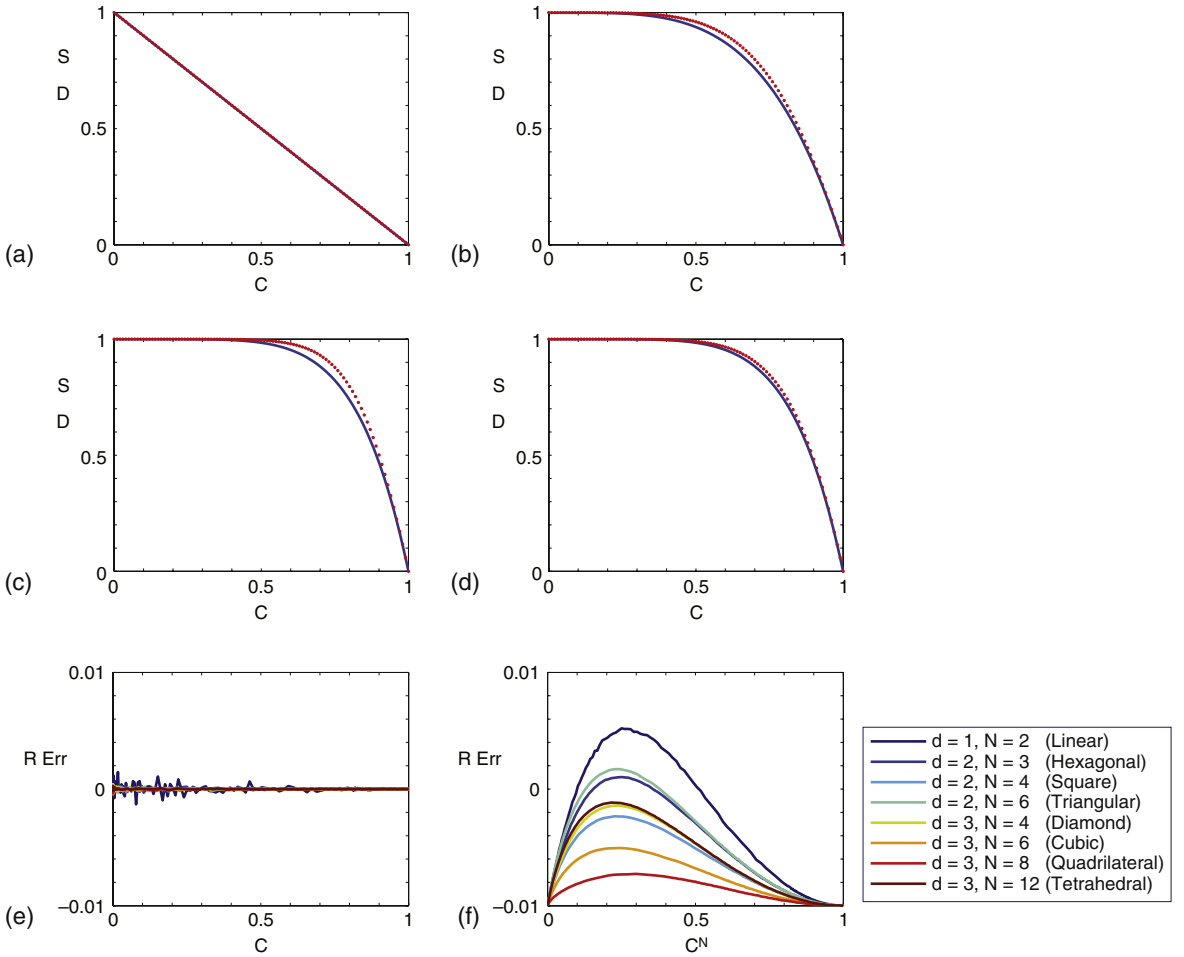

Fig. 1. Comparison of the slope of the MSD_x versus t curve. (a–d) Plots of slope $S = \mathrm{MSD}_x/2D_0t$ (red circles) and the expected value of $D(C)$ as a function of density C (blue line). The slope is determined by averaging over all agents up to $t = 1000$. (a) Blind agents on a triangular lattice. (b–d) Myopic agents on a square lattice, a triangular lattice (hexagonal tiling), and a simple cubic lattice, respectively. (e) Relative error versus density C for all blind walks. (f) Relative error versus C^N for myopic walks on various lattices, where N is the coordination number of the lattice. Color legend is for (e–f). (For interpretation of the references to colour in this figure legend, the reader is referred to the web version of this article.)

approximately 10^5 sites (e.g. 316×316 square lattice and $46 \times 46 \times 46$ cubic lattice). Every agent was tagged and its displacement from its starting position was recorded at each time. We determined the mean displacement of each agent and averaged over all agents; the mean magnitude was $\mathcal{O}(10^{-4})$, confirming that the mean displacement approximately zero. The net horizontal displacement as each time step was squared and summed. Averaging over all agents, the MSD_x was linear in time, and the slope depends on the crowd density C. We plot $\mathrm{MSD}_x/2D_0t$ and compare it with the expected value of $D(C)$ for various lattices. For blind agents, we confirm the linear nature of $D(C)$ in Eq. (11) (Fig. 1(a)), while for myopic agents, we confirm the nonlinear form of $D(C)$ in Eq. (11) is a very good fit, but some small errors appear and are largest for $C \sim 0.7$ (Fig. 1(b–d)).

We assess the relative error in the slope versus density over many different types of lattices. The relative error in the blind case is negligible (Fig. 1(e)); the fluctuations are larger for lower density since the simulations are averaged over a smaller number of agents than the higher density cases. The relative error in the myopic case increases from zero, reaches a maximum and then decreases to zero (Fig. 1(f)). Errors arise because of correlations in the occupancy (and consequently the vacancy) of nearest-neighbor sites. Such correlations were ignored when deriving transition probabilities $T(v|v')$, since independence of occupancy of neighboring sites was assumed. A vacant site in an agent's neighborhood may be due to the agent itself having recently created it in the previous move. Therefore, the probability of moving is higher than if the vacant sites were entirely random based on local density.

For the majority of the lattices considered, if an agent at site v moves to a vacant nearest-neighbor site $v' \in \mathcal{N}\{v\}$, then any of the other occupied sites $v'' \in N\{v\}$ can move into the vacated site v. At the next move the recently vacated site v'' is inaccessible to the agent at v', since it is not an element of $\mathcal{N}\{v'\}$; that is, $\mathcal{N}\{v\} \cap \mathcal{N}\{v'\} = \emptyset$. However, this is not the

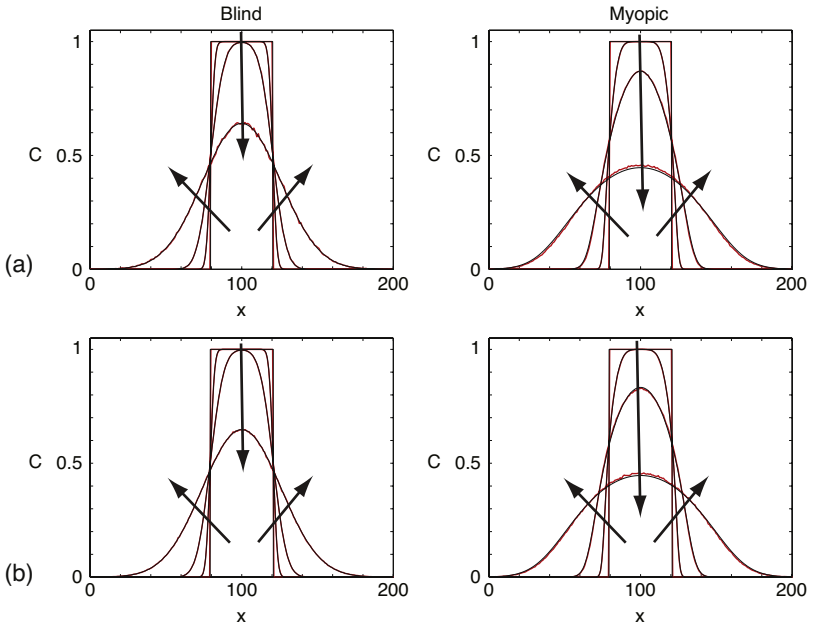

Fig. 2. Averaged column density data (red) compared with solutions to the PDE Eq. (4) (black) at times $t = 0, 10, 100, 1000$. Agents spread from $80 \leq x \leq 120$ on a 200×200 lattice, with probability of movement $P = 1$. Discrete results are averaged over 200 realizations. The left and right columns are for blind and myopic agents respectively. Arrows indicate the direction of increasing time. Row (a) square lattice. Row (b) triangular lattice (hexagonal tiling). (For interpretation of the references to colour in this figure legend, the reader is referred to the web version of this article.)

case for triangular ($d = 2, N = 6$) and tetrahedral ($d = 3, N = 12$) lattices, where $\mathcal{N}\{v\} \cap \mathcal{N}\{v'\} \neq \emptyset$, so the vacated site v'' may still be accessible to the agent at v'. Therefore, there is a higher correlation again between vacancy/occupancy of lattice sites. This is demonstrated in Fig. 1(f), where in general, for a fixed d, the relative error decreases as the number of nearest-neighbor sites N increases, except for two cases, namely the triangular and tetrahedral lattices.

5. Comparing discrete and continuum results

To test the validity of our averaging arguments, we generate and compare results from the discrete and continuum models for single and multiple species.

5.1. Single species

We consider a two-dimensional lattice, with spacing $\Delta = 1$, of size 200×200 with periodic boundary conditions imposed on the horizontal boundaries and reflecting boundary conditions (no flux) imposed on the vertical boundaries. All sites with $80 \leq x \leq 120$ are initially occupied with agents. This initial condition and the periodic boundary conditions reduce the system to a one-dimensional problem since no vertical structure is imposed by the initial agent distribution or the boundary conditions. Column-averaged density data is averaged over 200 identically prepared realizations.

For initial conditions which are independent of the vertical coordinate, the nonlinear diffusion equation, Eq. (4), reduces to a PDE with spatial derivatives in one variable. It is solved numerically with a finite difference method with constant grid spacing δx and implicit Euler stepping with constant time steps δt. Picard linearization, with tolerance ε, is used to solve the nonlinear equations. We used $\delta x = 0.05$ and $\delta t = 0.1$ and tolerance $\varepsilon = 1 \times 10^{-8}$. Our results are grid-independent.

The two columns in Fig. 2 illustrate results on a square and triangular lattice for blind (left column) and myopic (right column) agents. The blind results have been presented previously on a square lattice [9], but are included here for comparison purposes with myopic walkers. Comparison of the solution of Eq. (4) with column-averaged density profiles from the simulations shows an excellent correspondence between the two model solutions. The fit is slightly more accurate for blind walkers. As expected the myopic population spreads faster than the blind population, due to the larger diffusivity in the PDE and due to less aborted moves in the simulation. We checked results on several other types of two-dimensional lattices. On all lattices, the comparison between the continuum and discrete data is of comparable quality to the ones shown here.

To investigate more general initial conditions, it is appropriate to compare simulation results with a two-dimensional continuum model. We consider a 200×200 square lattice with spacing $\Delta = 1$, with reflecting boundary conditions (no flux) imposed on the horizontal and vertical boundaries. All sites with $80 \leq x, y \leq 120$ are initially occupied with agents. Site-averaged density data is averaged over 200 identically prepared realizations.

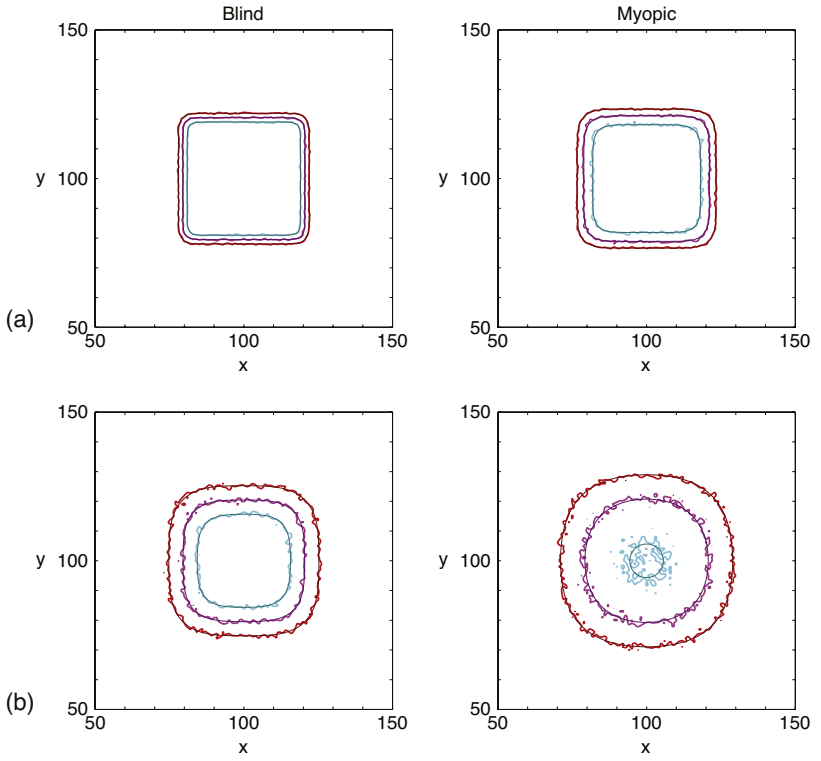

Fig. 3. Contours for the averaged density data and solutions to the PDE Eq. (4) at two times. Agents spread from $80 \leq x, y \leq 120$ on a 200×200 lattice, with probability of movement $P = 1$. The 0.25 (red), 0.5 (magenta) and 0.75 (cyan) contours for the discrete model are averaged over 200 realizations. The corresponding contours for the solution to Eq. (4) are shown (0.25, dark red; 0.5 dark magenta; 0.75, dark cyan). The left and right columns are for blind and myopic agents respectively. Row (a) $t = 10$. Row (b) $t = 100$. (For interpretation of the references to colour in this figure legend, the reader is referred to the web version of this article.)

For initial conditions which are dependent on both coordinates, the two-dimensional PDE Eq. (4) must be solved. An Alternating Direction Implicit (ADI) method is used. We used $\delta x = \delta y = 1$, $\delta t = 0.5$ and tolerance $\varepsilon = 1 \times 10^{-8}$. Our results are grid-independent.

Contours for the discrete and continuum results are superimposed and compare well (Fig. 3). Again, the results demonstrate that the myopic population spreads faster than the blind population.

5.2. Multiple species

We consider two subpopulations R (red) and G (green) on a square lattice, with spacing $\Delta = 1$, of size 200×200 with periodic boundary conditions imposed on the horizontal boundaries and reflecting boundary conditions imposed on the vertical boundaries. Three types of initial conditions are investigated.

- Scenario A: R population in $80 \leq x \leq 100$ at $C^{(\mathrm{R})} = 1$, while G population in $100 \leq x \leq 120$ at $C^{(\mathrm{G})} = 1$.
- Scenario B: R population in $80 \leq x \leq 120$ at $C^{(\mathrm{R})} = 1$, while the G population is in remaining region at $C^{(\mathrm{G})} = 0.5$.
- Scenario C: As in Scenario B, but both R and G populations at $C^{(\mathrm{R})} = 0.5$ and $C^{(\mathrm{G})} = 0.5$.

Only the blind results for Scenario B on a square lattice have been presented previously [9].

No vertical structure is imposed with these initial conditions and boundary conditions. Therefore, the nonlinear advection–diffusion equations (9) reduce to a system of PDEs with spatial derivatives in one variable only. The numerical scheme uses a finite difference method with Picard linearization for the diffusive term (treated implicitly), as described above, and higher order upwinding with flux limiting for the advection term (treated explicitly) [24]. We used $\delta x = 0.25$ and $\delta t = (\delta x)^2$ (blind), and $\delta t = (\delta x)^2/N$ (myopic) (to ensure that the Courant number is less than unity) and tolerance $\varepsilon = 1 \times 10^{-8}$. Our results are grid-independent.

First, simulations are performed for identical subpopulations, where $P^{(\mathrm{R})} = P^{(\mathrm{G})} = 1$. The averaged discrete results compare well with the corresponding solution to the continuum equations (9). Again the fit is slightly better for blind walkers than for myopic walkers (Fig. 4). The solution profiles in Scenario B exhibit features that are different from the other two scenarios. The density profiles for subpopulation G in Fig. 4(b) are nonmonotone with maximum values greater than the initial condition, and no maximum principle is obeyed. The nonmonotonicity appearing for both blind and myopic

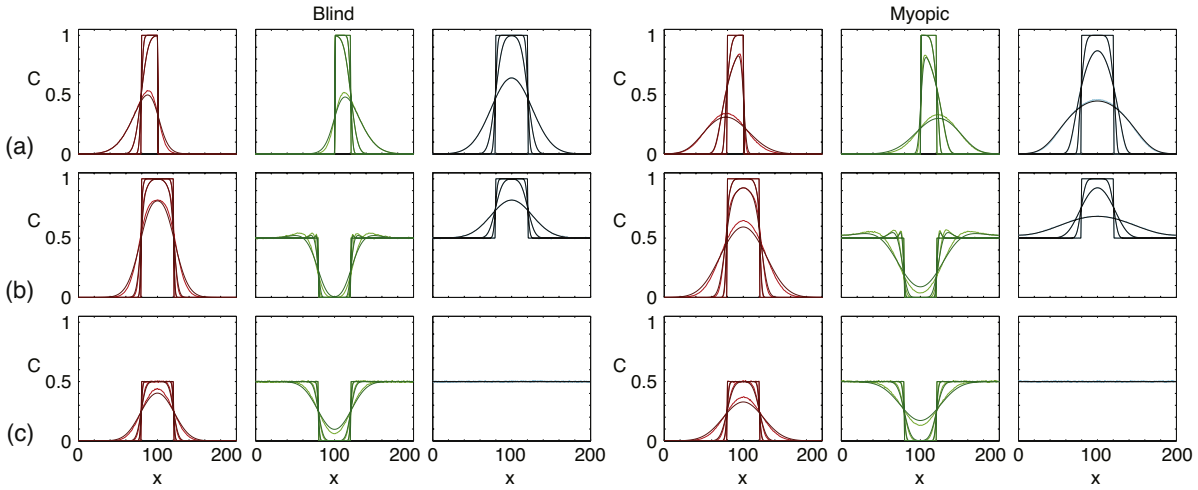

Fig. 4. Identical subpopulations R and G, with both populations move on average $P^{(R)} = P^{(G)} = 1$ times per timestep for three initial conditions, given by Scenario (A–C). The colors represent $C^{(R)}$ (red), $C^{(G)}$ (green) and total population $C = C^{(R)} + C^{(G)}$ (blue) for blind and myopic walkers. Row (a) Scenario A, Row (b) Scenario B, Row (c) Scenario C. Simulations are shown in lighter thick lines, with PDE solutions to Eq. (9) shown in darker fine lines. Simulations were performed on a square lattice measuring 200 × 200 and averaged over 200 realizations. Curves are shown for times $t = 0$, 10, 100, 1000 timesteps. (For interpretation of the references to colour in this figure legend, the reader is referred to the web version of this article.)

G agents is caused by exclusion effects. This scenario reveals subtleties that would not be apparent without the multispecies framework.

Secondly, simulations are performed for nonidentical subpopulations, where R and G have different motilities, with the three initial condition scenarios. The results in Fig. 5 follow the same trends as for the identical subpopulation case. Again nonmonotone solutions exist when there is a mismatch in the initial densities of the two subpopulations.

All simulations presented so far for multiple species are on a square two-dimensional lattice. We also investigated the performance of identical subpopulations on other types of lattices. Simulations were performed on various domains measuring approximately 200 in each dimension. (Slight differences in size occur because different lattice types have different spacings and therefore a different number of sites per area.) Average occupancies at positions along the x-direction were calculated by location for 1-d lattices, by column average for 2-d lattices, and by slice average for 3-d lattices. In order to compare results correctly, the probabilities of movement are scaled according to the dimension d of the lattice, namely as $P^{(R)} = P^{(G)} = d/3$, resulting in $D_0^{(R)} = D_0^{(G)} = 1/6$. This removes the dependence of the PDEs on d (Eq. (9)). Using the initial condition given by Scenario A, the results for the R subpopulation and the total population R+G are illustrated in Fig. 6 at $t = 100$. By symmetry, the G population is the mirror image of R reflected about the line $x = 100.5$, and is not shown. The results for blind agents all fall on the same curve for all lattice types, since the PDEs are independent of the lattice property N. For the myopic case, the curves are different for different values of N, as expected. Comparison between the averaged simulation data and the PDE is very good, as demonstrated in previous figures for the square lattice. Note that the PDE solutions should be independent of d and just a function of N. However, with different d and fixed N, there is an unavoidable disparity in the width of the initial condition imposed by the lattice geometry. This gives rise to slight differences in the PDE solution, due to differences in the initial density distribution. These are just discernible in Fig. 6, right column for $N = 4, 6$.

6. Discussion and conclusions

We have derived a partial differential equation which approximates well the average occupancy of the discrete agent-based model for myopic agents. This is a nonlinear diffusion equation, where the diffusivity depends on the number of nearest-neighbor sites, and therefore is lattice dependent. In contrast, the corresponding PDE description for blind agents is a linear diffusion equation, and therefore is the same for all lattices. In principle, experimental data could be used to determine the value of N, and therefore the type of lattice that is most appropriate to model individual systems. Tracking tagged agents, as well as fitting spatio-temporal population densities to solutions of a PDE, could be used to estimate a best fit for the parameter N. However, in some experimental systems, it may be difficult to distinguish any differences due to the noise in the experimental system.

We observe that the average discrete and continuum models match well for myopic agents, but the fit is not as good as the corresponding comparison with blind agents. The most likely explanation for this difference in behavior is a higher correlation between the occupancy of neighboring sites for a myopic random walk than for the blind random walk. We implicitly assume independence of occupancy of neighboring sites when deriving the conservation equations for these random walkers.

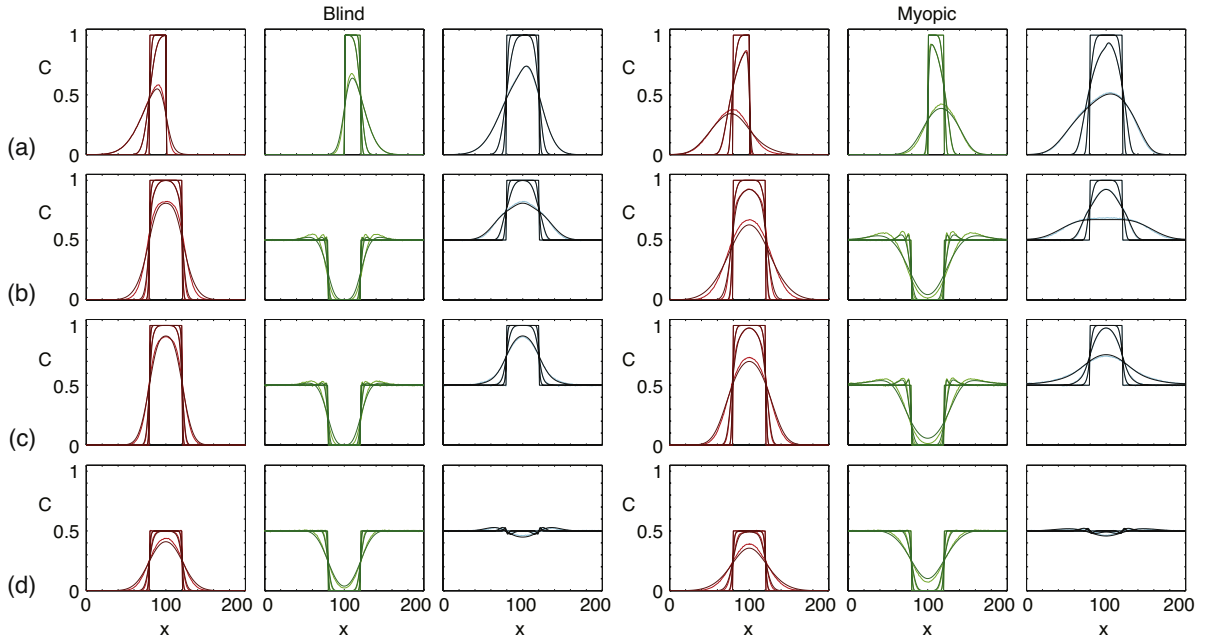

Fig. 5. Different subpopulations R and G for three initial conditions, given by Scenario (A–C). The colors represent $C^{(R)}$ (red), $C^{(G)}$ (green) and total population $C = C^{(R)} + C^{(G)}$ (blue) for blind and myopic walkers. Row (a) Scenario A with $P^{(R)} = 1$ and $P^{(G)} = 0.5$. Row (b) Scenario B with $P^{(R)} = 1$ and $P^{(G)} = 0.5$. Row (c) Scenario B with $P^{(R)} = 0.5$ and $P^{(G)} = 1$. Row (d) Scenario C with $P^{(R)} = 1$ and $P^{(G)} = 0.5$. Simulations are shown in lighter thick lines, with PDE solutions to Eq. (9) shown in darker fine lines. Simulations were performed on a square lattice measuring 200×200 and averaged over 200 realizations. Curves are shown for times $t = 0$, 10, 100, 1000 timesteps. (For interpretation of the references to colour in this figure legend, the reader is referred to the web version of this article.)

Different agent motility rules can give rise to the same PDE. An example of this is provided by the one-dimensional form of $\mathcal{D}(C) = 1 + 4C - 3C^2$ for myopic walkers. Fernando et al. [12] derived the same diffusivity function for agents with a contact-breaking interaction bias (case $\sigma = -1$). However, in this case, an agent does not move at all if it has no nearest neighbors. Therefore, the myopic agent rules are different from the contact-breaking rules, but they give rise to the same nonlinear diffusion equation. However, simulations for the contact interaction model do not fit well to the solution of the PDE. Such random walkers will always move away from others, and will cease to move once they have no neighbors. The resulting agent distribution patterns are a regular spacing of stationary agents. The behavior of myopic agents is quite different — isolated agents always move, and the PDE is a good approximation to the average discrete simulation results.

For the problem of the ant in the labyrinth [17–20], a single agent, the ant, performs a random walk, which may be either of the blind or the myopic type, along the open bonds of a realization of a Bernoulli percolation process. If the underlying percolation process is Bernoulli site percolation, then each site is "allowed" with probability p and a bond is open if and only if both sites that it links are allowed. If $p < p_c$, where p_c is the percolation threshold, all clusters are finite with probability one, the ant is trapped on a finite island, and its mean square displacement saturates at long time at a value determined by the cluster size and shape. In contrast, for $p > p_c$, the ant undergoes a diffusion process with a p-dependent diffusivity, provided that it starts on the infinite cluster.

For the interacting agent models considered in the present paper, each agent plays the role of an ant in a labyrinth, where the paths of allowed sites though the labyrinth consist of sites not occupied by other agents. The other agents essentially constitute the walls of the labyrinth. However, the labyrinth seen by a given agent evolves over time and therefore no agent is ever trapped in a finite region of space for an indefinite period.

In cellular systems, individual cells extend filopodia to gather environmental cues and gain an awareness of neighboring cells. Since cells exclude volume, the simple rules introduced for myopic agents in a crowd of myopic agents allows the nature of such interactions to be taken into account. Common forms of contact-mediated migration, as observed in neural crest cells [25–27], can be described a myopic random walk.

This work shows that transport coefficients extracted from tracking an individual cell or agent, namely $D(C)$, does not describe the global behavior of the population, which is governed by the diffusivity $\mathcal{D}(C)$. However, representing a single population as two or more identical subpopulations gives insights into the nature of the agent interactions, as in Simpson et al. [9]. Using a multispecies formulation, a relationship between $\mathcal{D}(C)$ and $D(C)$ is extracted. Furthermore, the difference between the two functions is given by $CV(C)$, where $V(C)$ arises from the advection term in the PDE governing the identical subpopulations.

Consideration of subpopulations is not only a revealing theoretical technique. It also has application in recent neural crest cell invasion experiments. Either a subpopulation of donor cells is placed within a subpopulation of host cells and

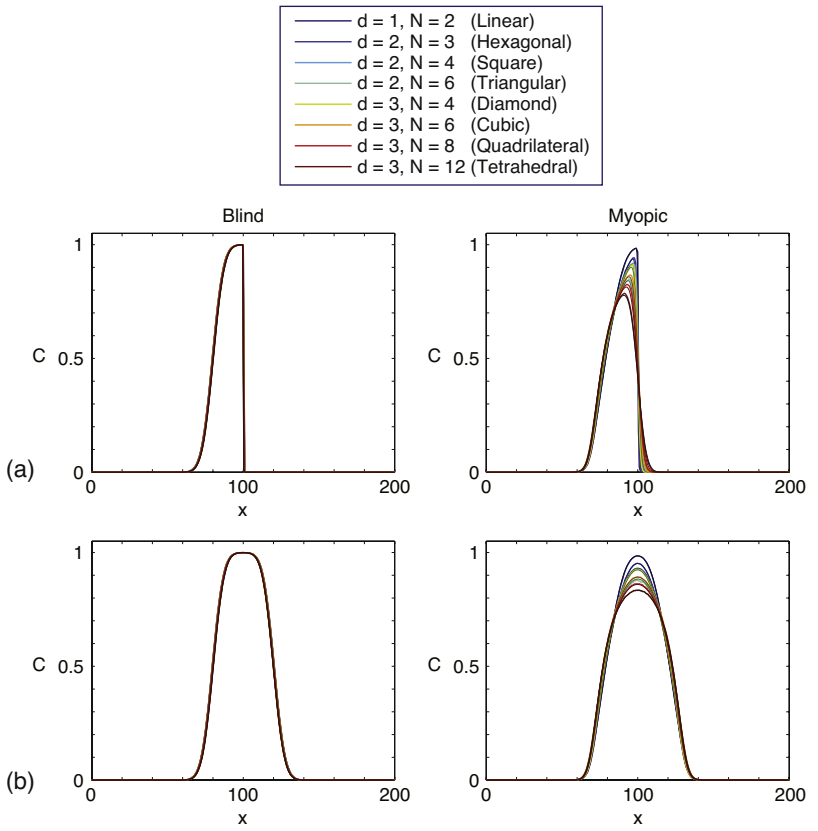

Fig. 6. Multiple lattice types with Scenario A. Row (a) $C^{(R)}$ population. Row (b) Total population $C = C^{(R)} + C^{(G)}$. Simulations were performed on various lattices measuring approximately 200×200 averaged over 200 realizations. Here $P^{(R)} = P^{(G)} = d/3$. Simulations are shown in lighter thick lines, with PDE solutions to Eq. (9) shown in darker fine lines. The left and right columns are for blind and myopic agents at $t = 100$ respectively. Color legend is for all figures. (For interpretation of the references to colour in this figure legend, the reader is referred to the web version of this article.)

different antibodies identify each subpopulation [28] or a photoconvertible fluorescent protein is expressed by all cells and photoconversion is used to identify a selected subpopulation [29]. The blind and myopic multispecies models developed and investigated here assist with the interpretation of these kinds of experimental data.

Acknowledgments

This work was supported by a grant from the Australian Research Council to Kerry Landman. Kerry Landman is an ARC Professorial Fellow. We thank Professor Barry Hughes for helpful discussions, as well as Maddy Huggins, an undergraduate student, who performed some preliminary simulations.

References

[1] T.M. Liggett, Stochastic Interacting Systems: Contact, Voter and Exclusion Processes, Springer-Verlag, Berlin, 1999.
[2] F. Spitzer, Adv. Math. 5 (1970) 256–290.
[3] A. Schadschneider, Physica A 313 (2002) 153–187.
[4] A. John, A. Schadschneider, D. Chowdhury, K. Nishinari, J. Theor. Biol. 231 (2004) 279–285.
[5] L.M. Sander, T.S. Deisboeck, Phys. Rev. E 66 (2002) 051901.
[6] M.J. Simpson, A. Merrifield, K.A. Landman, B.D. Hughes, Phys. Rev. E 76 (2007) 021918.
[7] M.J. Simpson, K.A. Landman, B.D. Hughes, Bull. Math. Biol. 71 (2009) 781–799.
[8] M.J. Simpson, K.A. Landman, B.D. Hughes, Phys. Rev. E 79 (2009) 031920.
[9] M.J. Simpson, K.A. Landman, B.D. Hughes, Physica A 388 (2009) 399–406.
[10] C. Deroulers, M. Aubert, M. Badoual, B. Grammaticos, Phys. Rev. E 79 (2009) 031917.
[11] D. Fanelli, A.J. McKane, Phys. Rev. E 82 (2010) 021113.
[12] A.E. Fernando, K.A. Landman, M.J. Simpson, Phys. Rev. E 81 (2010) 011903.
[13] K.J. Painter, Bull. Math. Biol. 71 (2009) 1117–1147.
[14] M.J. Simpson, K.A. Landman, B.D. Hughes, A.E. Fernando, Physica A 389 (2010) 1412–1424.
[15] T.P. Witelski, Appl. Math. Lett. 8 (1995) 27–32.
[16] K.A. Landman, L.R. White, Phys. Fluids 23 (2011) 012004.
[17] B.D. Hughes, Random Walks and Random Environments, vol. 2, Oxford University Press, Oxford, UK, 1995.

[18] C.D. Mitescu, J. Roussenq, in: G. Deutscher, R. Zallen, J. Adler (Eds.), Percolation Processes and Structures, Adam Hilger, Bristol, Ann. Israel Phys. Soc. 5 (1983), 81–100.
[19] I. Majid, D. Ben-Avraham, S. Havlin, H.E. Stanley, Phys. Rev. B 30 (1984) 1626–1628.
[20] D. Stauffer, A. Aharony, Introduction to Percolation Theory, Taylor and Francis, London, 1991.
[21] D. Chowdhury, A. Schadschneider, K. Nishinari, Phys. Life Rev. 2 (2005) 318–352.
[22] B.D. Hughes, Random Walks and Random Environments, vol. 1, Oxford University Press, Oxford, UK, 1995.
[23] E.A. Codling, M.J. Plank, S. Benhamou, J. R. Soc. Interface 5 (2008) 813–834.
[24] R.J. Leveque, Numerical Methods for Conservation Laws, Birkhauser, Basel, 1992.
[25] H.M. Young, A.J. Bergner, R.B. Anderson, H. Enomoto, J. Milbrandt, D.F. Newgreen, P.M. Whitington, Dev. Biol. 270 (2004) 455–473.
[26] N.R. Druckenbrod, M.L. Epstein, Dev. Biol. 287 (2005) 125–133.
[27] P.M. Kulesa, C.M. Bailey, J.C. Kasemeier-Kulesa, R. McLennan, Dev. Biol. 344 (2010) 543–554.
[28] M.J. Simpson, D.C. Zhang, M. Mariani, K.A. Landman, D.F. Newgreen, Dev. Biol. 302 (2007) 553–568.
[29] P.M. Kulesa, J.M. Teddy, D.A. Stark, S.E. Smith, R. McLennan, Dev. Biol. 316 (2008) 275–287.